Instrumental Receiver Bias Estimation for Ionospheric Total Electron Content by Neural Network Model

Phyo C Thu[1†], **Pornchai Supnithi**[1], **Jirapoom Budtho**[1], **Apitep Saekow**[2], **Thanomsak Sopon**[3], **Kornyanat Hozumi**[4], and **Lin Min Min Myint**[1], Non-members

ABSTRACT

Total Electron Content (TEC) is one of the most important parameters in the study of the ionosphere, especially for determining ionospheric disturbances. The TEC levels are typically estimated from dual-frequency GPS observation data. Since the measured TEC contains discrepancies such as satellite and receiver biases, they need to be removed to obtain more accurate TEC values. In this work, we estimate the receiver bias using a neural network technique. Based on the exhaustive evaluation, we design a neural network (NN) model with two-hidden layers, and it is trained with datasets from three GNSS observation stations in Thailand. The prediction from the proposed neural network deviates from the baseline reference using the minimum standard deviation method with significantly faster computational time. The trained NN model is also tested for estimating the receiver bias values at other untrained stations in Thailand.

Keywords: Total Electron Content, Receiver Bias, Global Positioning System, Ionospheric Delay, Neural Network

1. INTRODUCTION

The ionosphere is an ionized region at 50-1500 km above the earth's surface. The ionosphere is an important layer for high frequency (HF), very high frequency (VHF) and ultra high frequency (UHF) radio signal propagations, including the Global Navigation Satellite System (GNSS) [1] because it can absorb or bend the radio waves as well as reflect the signals. Total electron content (TEC), with the unit of TECU (1 TECU = 10^{16} electron/m^2), is used as one of the important parameters for studying and monitoring ionospheric behavior and disturbances. The TEC is typically estimated from a linear combination of GNSS signals of two frequencies; for example, in GPS, the code and carrier phase signals of two L-band frequencies 1575.42 MHz (f1) and 1227.70 MHz (f2) [2]. The computed TEC from observation data, however, includes not only the ionospheric TEC, but also the offsets caused by the internal electronic circuit of the GPS satellites, known as satellite bias, and by ground receivers known as receiver bias [3]. In order to obtain more accurate TEC values, these bias values need to be estimated and removed from the raw TEC. Although the satellite bias can be obtained from GNSS data service providers such as the International GNSS Service (IGS) [4], the receiver bias values still need to be estimated using the GNSS observed data.

To estimate the receiver bias, various approaches have been proposed in the literatures [4-8]. In [5], the instrumental bias is computed by combining the biased ionospheric terms from all the available receiver stations in the Kalman filter process. In this case, the coefficients of the polynomial terms for each station are treated as random walk stochastic processes, and the bias is considered as constant for the entire period (24 hours). Because of the time variation of the instrumental bias, frequent calibration or reestimation is required.

In [4], the researchers attempted to estimate both TEC and receiver bias for several equatorial and low latitude GNSS observation stations in IGS and GPS Aided Geo Augmented Navigation (GAGAN). They implement a five-state Kalman Filter to estimate the receiver bias. After choosing the initial receiver bias value, a modified fitted receiver bias (FRB) method is applied to improve the receiver bias estimation. However, this work considered only nighttime data in estimating receiver bias with the FRB method because TEC variations are relatively small during nighttime.

In [6], least-square fitting technique is used to derive the instrumentation bias from the collected data from GPS Earth Observation Network (GEONET) over 1,000 GPS-receiver stations in Japan, and then the minimum summation of the TEC standard deviation method for the single GPS-receiver bias estimation is also presented by considering that vertical TEC from lower elevation angles is similar to vertical TEC from higher elevation angles. This method is simple and sufficiently accurate

Manuscript received on May 5, 2023; revised on July 7, 2023; accepted on August 18, 2023. This paper was recommended by Associate Editor Piya Kovintavewat.

[1]The authors are with School of Engineering, King Mongkut's Institute of Technology Ladkrabang, Bangkok 10520, Thailand.

[2]The author is with Stamford International University, Bangkok 10520, Thailand.

[3]The author is with Rajamangala University of Technology Isan, Nakhon Ratchasima 30000, Thailand.

[4]National Institute of Information and Communication Technology, Koganei, Tokyo, 184-8795, Japan.

[†]Corresponding author: 64601010@kmitl.ac.th

Digital Object Identifier: 10.37936/ecti-eec.2023213.251470

to estimate receiver bias for computing the absolute TEC according to their observation in GEONET.

Moreover, the researchers apply the minimum standard deviation method to estimate the receiver bias to get the absolute TEC value in [7]. The paper highlights that the receiver bias values may not be the same throughout the day. The gradient descent algorithm is used for deriving the receiver bias over the GNSS observation data in Thailand in [8] and the results show that the computational time is faster than the minimum summation of TEC standard derivation methods with an accuracy deviation of less than 10 percent. Alternatively, the singular value decomposition (SVD) method is employed to eliminate the receiver bias in Korea GPS network stations [9] and in stations over China [10].

However, all these estimation methods require long computational time to estimate the receiver bias. While neural networks have been intensively applied to predict TEC in [11] as well as the TEC forecasting models for low-latitude regions described in [12] and [13], limited research has been conducted on the application of neural networks for receiver bias determination, with only one known study conducted in Japan [14].

In this work, we develop a neural network with the Levenberg-Marquart algorithm to predict the receiver bias as an alternative approach. We implement a neural network model with 2 hidden layers based on the dataset of three GNSS stations over the Thailand region and then evaluate the performances of the designed neural network model in a comparison with the reference method [6]. The trained model is also tested to compute the receiver bias values at other untrained stations. The train neural network model can provide the receiver bias with faster processing time compared to the reference method as well.

2. TOTAL ELECTRON CONTENT (TEC) COMPUTATION

2.1 Total Electron Content (TEC)

Slant total electron content (STEC) is defined as the density of electrons along the line-of-sight path between a satellite and a receiver in the ionosphere layer[15] as shown in Fig. 1. At a single location, the STEC varies due to elevation angles of satellites as well as the time of day. To compute the STEC, we employ the geometric-free combination of code and carrier phase pseudorange of two frequencies, in GPS [12].

Based on the GPS signals, STEC can be obtained as the difference between the pseudorange (P_1 and P_2), $STEC_P$ and the difference between the carrier phases (L_1 and L_2), $STEC_L$, of the dual L-band frequencies [16], i.e.,

$$STEC_P = \frac{2f_1^2 f_2^2}{k(f_1^2 - f_2^2)}(P_2 - P_1), \qquad (1)$$

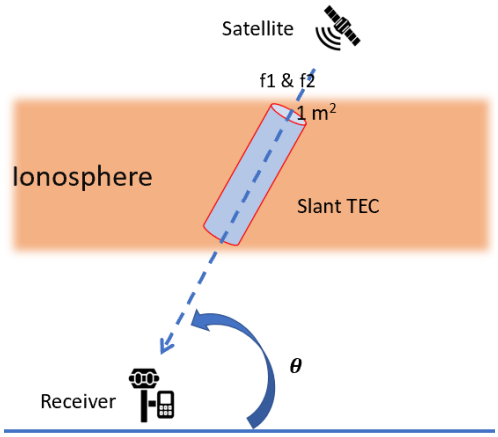

***Fig. 1**: Slant total electron content (STEC) illustration.*

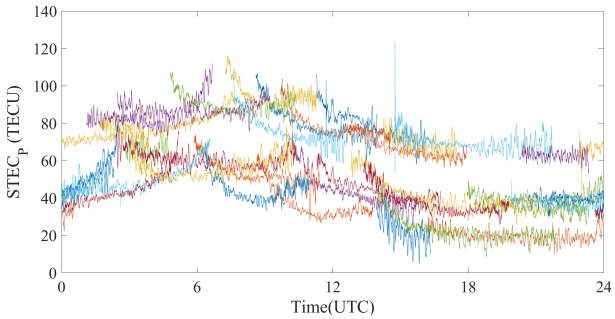

***Fig. 2**: Example of raw STEC from code pseudorange of KMIT observation station on DOY 001, 2021.*

and

$$STEC_L = \frac{2f_1^2 f_2^2}{k(f_1^2 - f_2^2)}(L_1\lambda_1 - L_2\lambda_2), \qquad (2)$$

where k is related to ionospheric refraction (80.62 m^3/s^2), f_1 = 1575.42MHz, and f_2 = 1227.60 MHz, λ_1 and λ_2 are the wavelengths with respect to f_1 and f_2, respectively. An example of raw STEC from code pseudorange measurement of the KMIT observation station on DOY 001, 2021 is shown in Fig. 2. Similarly, Fig. 3 shows the raw STEC from carrier phase measurements of the KMIT station on the same day.

As we can see in Figs. 2 and 3, the levels of STEC from code pseudorange ($STEC_P$) are relatively noisy while the variations of STEC from carrier-phase ($STEC_L$) are smooth. In general, $STEC_L$ is more precise, smoother, and less sensitive to multipath than$STEC_P$, although it contains integer ambiguity due to cycle slip issue The $STEC_L$ is then adjusted to the $STEC_P$ levels with phase leveling [17], to obtain adjusted STEC, $STEC_{adj}$,i.e.,

$$STEC_{adj} = STEC_L + \overline{STEC_P + STEC_L}, \qquad (3)$$

where $\overline{STEC_P - STEC_L}$ is the mean of the difference between $STEC_P$ and $STEC_L$. An example of the adjusted STEC after phase leveling on DOY 001, 2021 is shown in Fig. 4.

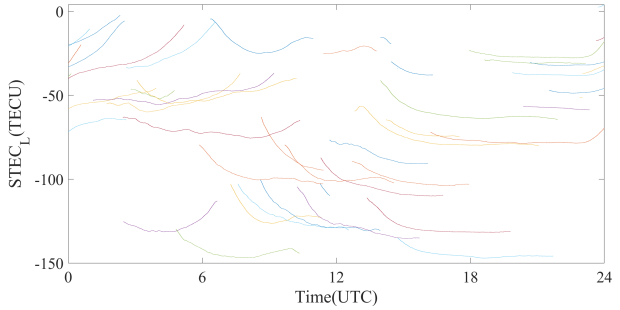

***Fig. 3**: Example of raw STEC from the carrier-phase measurement of KMIT observation station on DOY 001, 2021.*

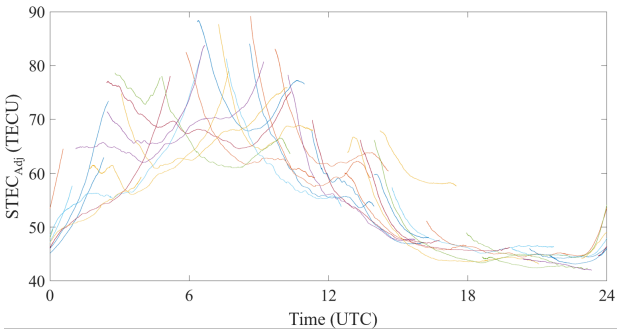

***Fig. 4**: Example of carrier-phase STEC after levelling to code-STEC at KMIT station on DOY 001, 2021.*

The STEC can then be converted to vertical total electron content (VTEC) which is the density of electrons in the ionosphere along the vertical path as shown in Fig. 5. VTEC can be calculated by multiplying with the slant factor with respect to the elevation angles of satellites based on the Single Layer Ionospheric Model (SLIM) [6], i.e.,

$$VTEC = STEC_{adj} \cos x, \tag{4}$$

where $\cos x$ is the slant factor related to elevation angles of GPS satellites which can be computed from

$$\cos x = \sqrt{1 - (\frac{R_E}{R_E + h_{iono}} \cos \theta)^2}, \tag{5}$$

where R_E is the radius of the earth (6,378,137 meters in WGS84 standard), h_{iono} is the assumed height of the ionosphere at 350 km, and θ is the elevation angle of the satellite as shown in Fig. 5.

Since, in reality, the STEC contains inherent delays from satellite bias and receiver bias as discussed in the previous section, the VTEC without instrumental satellite bias and receiver bias can be expressed as

$$VTEC = (STEC_{adj} - B_s - B_r) \cos x, \tag{6}$$

where B_s is the satellite bias and B_r is the receiver bias. The satellite bias of the GPS satellites can be obtained from the International GNSS Service (IGS) by the Center of Orbit Determination in Europe (CODE) [18] and the

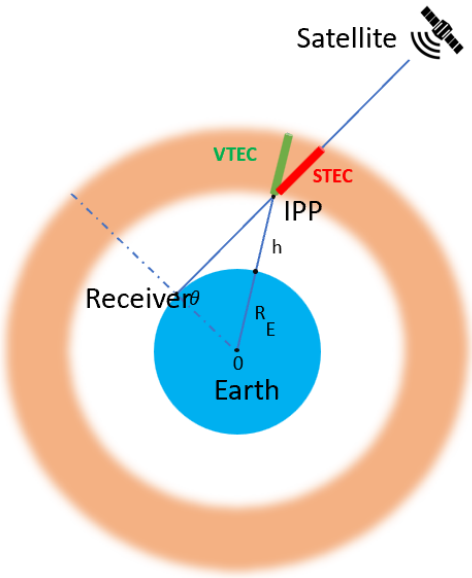

***Fig. 5**: Conversion of vertical total electron content from slant total electron content based on SLIM.*

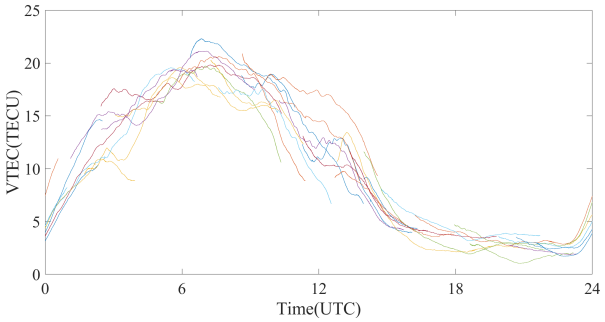

***Fig. 6**: Example of VTEC after removing the instrumental bias (satellite and receiver bias) of the KMIT observation station on DOY 001, 2021.*

receiver bias still needs to be estimated based on these computed adjusted STEC from Eq. (3) after removing the satellite bias.

2.2 Receiver Bias Computation

Firstly, we review the minimum standard deviation method [16] which is a well-known approach to estimate the receiver bias of a single receiver. The computed receiver bias from this method is used as the baseline solution and the target values during training and testing the NN model. In this method, the receiver bias is derived after the satellite bias is removed from the adjusted STEC. It is assumed that the VTEC with the low elevation angles should not be different from the VTEC computed from high elevation angles since VTEC is computed from the GPS observation of all satellites. The sum of the standard deviation of VTEC (σ_{Total}) will be minimized when we select the appropriate receiver bias. It can be computed

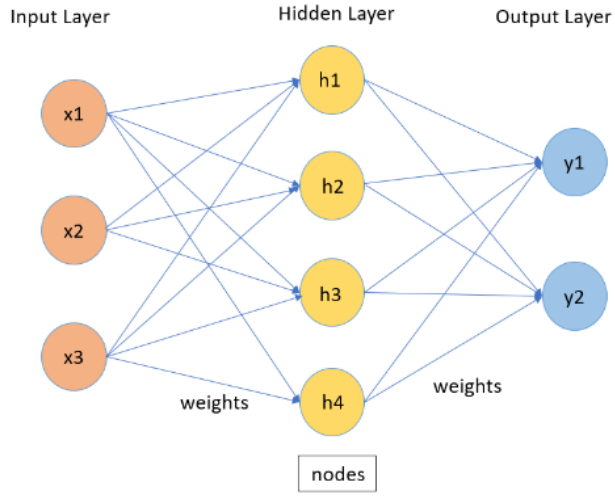

***Fig. 7**: Structure of a neural network model.*

from [8]

$$\sigma_{Total} = \sum_{j=1}^{N_t} \sigma_{VTEC,j}, \tag{7}$$

where N_t is the number of visible satellites at the same time and standard deviation of VTEC ($\sigma_{VTEC,j}$) at time j is

$$\sigma_{VTEC,j} = \sqrt{\frac{1}{N_{sat,j}} \sum_{i=1}^{N_{sat,j}} (VTEC_{j,i} - \overline{VTEC_j})^2}, \tag{8}$$

where $N_{sat,j}$ is the number of satellites at time j, $VTEC_{j,i}$ is the VTEC of the i^{th} satellite at time j and $\overline{VTEC_j}$ is the mean of the VTEC of visible satellites at time j.

To estimate the receiver bias, various receiver bias values are applied for converting the STEC to VTEC with respect to Eq. (6). After that, the standard deviation of the VTEC is computed, and the receiver bias value which can give the minimum standard deviation of VTEC is assumed to be the correct receiver bias based on Eqs. (6) and (7). An example of VTEC after removing receiver bias is shown in Fig. 6. We will be using this method as a reference method.

3. NEURAL NETWORK METHOD

Neural networks are artificial adaptive systems inspired by the human brain's operations [19]. Neural networks are made up of three node layers: input layer, output layer, and hidden layers and each node connects to others with weight and bias values. Currently, various types of NN have been considered including deep learning, recurrent neural network (RNN), and long short-term memory network (LSTM) among others. However, in this work, we consider a simple NN model as shown in Fig. 7.

The neural network node contains input data: x, weights: w, bias: b, and output: y. Neural networks can be viewed as highly non-linear functions with the basic form as

$$F(x, w) = y, \tag{9}$$

where w is generally ordered by the weights of each neuron plus each bias, i.e.,

$$\sum_{i=1}^{m} w_i x_i + b = w_1 x_1 + w_2 x_2 + ... + w_n x_n + b, \tag{10}$$

By modifying the weight and bias values to minimize network errors, neural network learning is essentially a function of the optimization problem.

3.1 Levenberg-Marquardt Algorithm

The Levenberg-Marquart algorithm (LM) is the damped-least square (DLS) method which provides a numerical solution to the problem of minimizing a function (usually non-linear) function throughout the space of parameters in the function [20]. The Levenberg-Marquart includes solving the equation, i.e.,

$$(\mathbf{J}^t\mathbf{J} + \eta\mathbf{I})\boldsymbol{\delta} = \mathbf{J}^t\mathbf{E}, \tag{11}$$

where $\mathbf{J}$ is the Jacobian matrix for the system, η is the Levenberg's damping factor, and $\boldsymbol{\delta}$ is the weight update vector which is adjusted at each iteration and guides the optimization process. The error vector $\mathbf{E}$ contains the output errors for each input vector. It is derived using the mean square error (MSE), i.e.,

$$MSE = \frac{1}{n} \sum_{i=1}^{n} (y_i - \tilde{y}_i)^2, \tag{12}$$

where n is the number of data points, y_i is the actual value, and $\tilde{y}_i$ is the predicted value.

The Jacobian matrix is an N-by-W matrix of all first-order partial derivatives of a vector-valued function where N is the number of entries in the training set and W is the total number of parameters (weights + biases) of our network. It is obtained by taking partial derivatives of each output in terms of each weight, i.e.,

$$\mathbf{J} = \begin{pmatrix} \frac{\partial F(x_1,\omega)}{\partial F\omega_1} & \cdots & \frac{\partial F(x_1,\omega)}{\partial F\omega_w} \\ \vdots & \ddots & \vdots \\ \frac{\partial F(x_N,\omega)}{\partial F\omega_1} & \cdots & \frac{\partial F(x_N,\omega)}{\partial F\omega_w} \end{pmatrix}, \tag{13}$$

where $F(x_i, \omega)$ is the network function evaluated for the i^{th} input vector of the training set using the weight vector $\mathbf{w}$ and ω_j is the j^{th} element of the weight vector $\mathbf{w}$ of the network.

The Hessian matrix $\mathbf{H}$ does not need to be calculated based on least-squares like LM. It can be estimated from the Jacobian matrix, i.e.,

$$\mathbf{H} \approx \mathbf{J}^t\mathbf{J}, \tag{14}$$

A small value such as 0.1 would be used as starting point for η. Then, the Levenberg-Marquardt equation

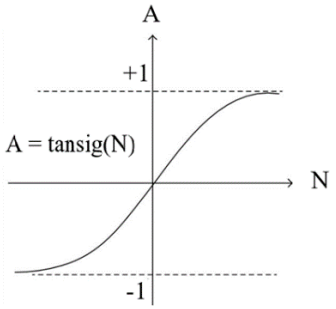

***Fig. 8**: Hyperbolic tangent sigmoid transfer function.*

is solved with the LU decomposition. The weights **w** is updated using $\boldsymbol{\delta}$ and network errors for each entry in the training set are computed once the equation is solved. When the new sum of squared errors is smaller, η is smaller and the iterations finish. Otherwise, the new weights are discarded, and the method is repeated with a higher value for η. There are some variations in the algorithm, but it is the same method implemented internally by the MATLAB Deep Learning Toolbox [21] which is used during this study.

3.2 Hyperbolic Tangent Sigmoid Transfer Function

The hyperbolic tangent sigmoid transfer function, often known as "tansig," is used in this study for its speed in the backward-propagation algorithm. It is a non-linear transfer function for neural network optimization. The output of a layer is computed using a transfer function based on its input.

As shown in Fig. 8, $A = tansig(N)$ takes an N and returns the A of the elements of N squashed into (-1 -1) [22]. It calculates output as,

$$A = \frac{2}{1 + e^{-2N}} - 1. \tag{15}$$

3.3 Neural Network Design

In this proposed NN model, we use the STEC data from 7 satellites, the minimum number of visible satellites for the entire time as the input, and the output of the model is a single receiver bias value. We design an NN model with 2 hidden layers as shown in Fig. 9. To find the optimum number of neurons, the network is investigated for various number of hidden neurons ranging from 10 to 60 in each layer. The same number of neurons is used in each layer for simplicity. Assuming that the receiver bias is fixed, or its variation is negligibly small within 12-hour of daytime and nighttime, the mean value of the 12-hour prediction of receiver bias will be used as the final output.

3.4 Datasets

In this study, we try to predict the receiver bias from STEC after the satellite bias is already removed. For the target values, the receiver bias datasets for each station

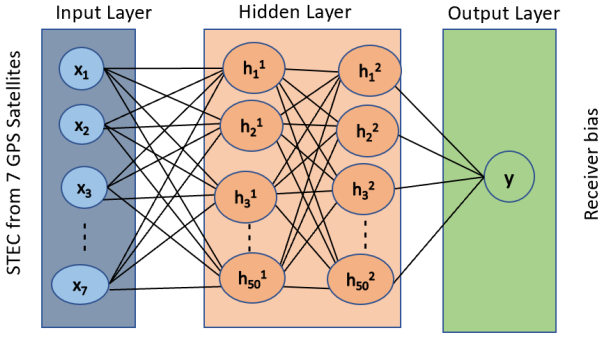

***Fig. 9**: Neural networks design used in this study.*

***Table 1**: Coordinates of 3 GNSS observation stations where data are used in the neural network training.*

Stations	Locations	Duration
KMIT	Lat: 13.6394° N Long: 100.772° E	Jan 1, 2018 – Dec 31, 2020
STFD	Lat: 13.6471° N Long: 100.661° E	Jan 1, 2018 – Dec 31, 2020
RUTI	Lat: 14.893° N Long: 102.120° E	Jan 1, 2018 – Dec 31, 2020

are computed separately at daytime (UTC 00:00 to 12:00 hr at 7:00 am to 7:00 pm local time) and nighttime (UTC 12:00 to 24:00 hr at 7:00 pm to 7:00 am local time) using the minimum standard deviation method [6]. For the NN model, STEC is used as the input dataset while receiver bias is the output. The STEC and receiver bias datasets with 5-minute resolution for 3 years are prepared from 3 stations within Thailand as shown in Table 1. The locations of the receiver stations are shown in Fig. 10. Fig. 4 shows the example of 1-day STEC datasets before removing the receiver bias and Fig. 11 shows the example of a 1-day receiver bias dataset. The receiver bias values for daytime and nighttime are computed separately. The receiver bias values are high during the daytime, but become low during the nighttime. However, we cannot see each satellite for the whole day as it orbits the earth approximately twice a day. So, there are some NaN values in the STEC dataset while the receiver cannot see the satellites. So, we only use the STEC based on the minimum numbers of visible satellites in order to eliminate the NaN values. In this work, we select STEC of 7 visible satellites at each time sorted by ascending PRN. During this study process, datasets are randomly divided into 75 percent for training, 15 percent for validation, and 10 percent for testing, respectively.

4. RESULTS AND DISCUSSIONS

In this work, the neural network is trained with the STEC and receiver bias datasets from 2018 to 2020 from 3 stations. After that, STEC datasets from some days in 2021 are used to predict the receiver bias in testing and the results are analyzed by comparing the estimated

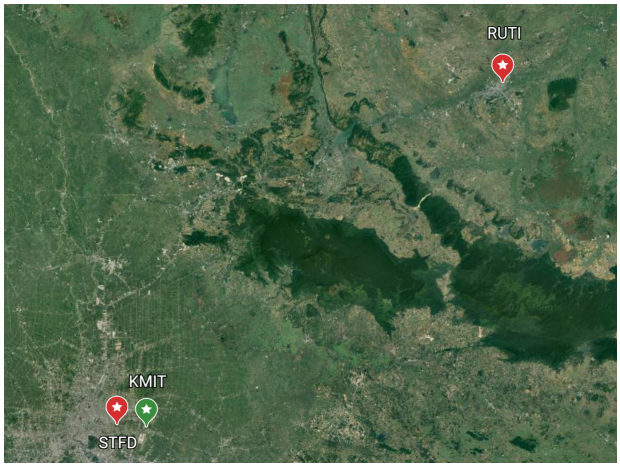

***Fig. 10**: Location of 3 GNSS observation stations used in training of neural network.*

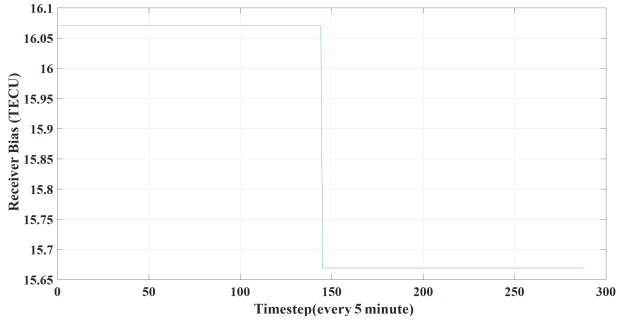

***Fig. 11**: Example of 1-day receiver bias datasets from KMIT station on DOY 001, 2021.*

receiver bias using the reference method.

4.1 Training Results

Firstly, the performances of the neural network with 2 hidden layers are investigated with 10, 20, 30, 40, 50, and 60 neurons in each hidden layer on the datasets from the KMIT station. The performances of neural networks with different numbers of neurons in each layer are shown in Fig. 12. According to the results, the NN model with 50 neurons in each hidden layer gives the lowest mean square error (MSE) and there is no noticeable improvement after 50 neurons. Therefore, the neural network model with two hidden layers in which 50 neurons in each hidden layer are considered in this study.

To check the training performance of the model, we examine the regression of the training between the target receiver bias and the predicted receiver bias which is found during training on the datasets of KMIT, RUTI, and STFD stations as shown in Fig. 13. We notice that the trained model provides the highest regression on STFD station with R = 0.94432 and but lowest regression on KMIT station with R = 0.86309.

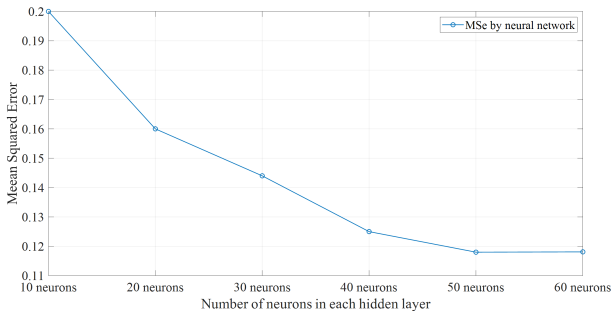

***Fig. 12**: Performance of the neural networks with different numbers of neurons in each hidden layer at the KMIT station.*

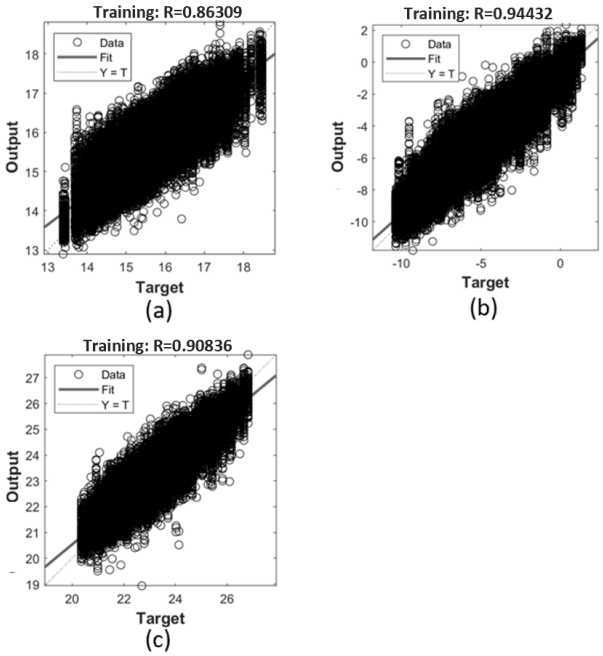

***Fig. 13**: Training regression between the target receiver bias and the predicted receiver bias on the dataset of (a) KMIT station, (b) STFD station, and (c) RUTI stations by using the neural network approach.*

4.2 Prediction Results

We investigate the prediction results from the neural network model with the testing dataset. The prediction results of the neural network model from three stations (KMIT, STFD, and RUTI) included in the study are shown in Fig. 14. The x-axis represents the timesteps in every 5-minute and the y-axis represents the percentages of errors which deviate from the reference method computed by

$$Error(\%) = \left| \frac{B_{R,NN} - B_{R,REF}}{B_{R,REF}} \right| \times 100, \qquad (16)$$

where $B_{R,NN}$ is the estimated receiver bias from neural network model and $B_{R,REF}$ is the receiver bias from reference method, respectively.

The neural model shows the capability to predict

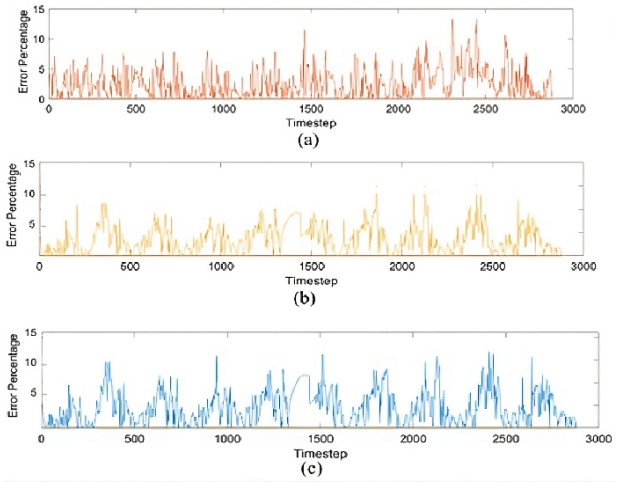

***Fig. 14**: Percentage of errors during the testing from (a) KMIT station (b) STFD station and (c) RUTI station.*

receiver bias at different stations and most of the errors are less than 10 percent from the reference method in all three stations although there are some spikes.

In addition, one-day data from various seasons of the year 2021 are selected as DOY 80 for the vernal equinox, DOY 172 for the summer solstice, DOY 266 for the autumnal equinox, and DOY 356 for the winter solstice, respectively, to test the prediction performances of the neural network models. We test the neural network model with the KMIT station which is included in the training data as well as the AER1 station which is not included in the training data. Since we want the receiver bias in 12-hour resolution, the mean value of the 12-hour prediction of receiver bias will be used to compare with the reference method for daytime and nighttime. Fig. 15 shows the trend of receiver bias from the reference method and receiver bias from neural network models at the KMIT station during testing. The prediction values are close to the reference method, and it also shows high values during the daytime and low value during the nighttime. Fig. 16 shows the percentages of errors that deviated from the baseline reference method. We can see that the predicted receiver bias from the neural network approach can follow the trend of the reference method quite well with a deviation of less than 5 percent.

We also analyze the effects of receiver bias estimation errors by the neural network on the vertical total electron content (VTEC). We compute the VTEC by using the receiver bias from the neural network based on Eq. (4). The maximum deviation of VTEC on each day by using the receiver bias from neural network approaches compared to the reference method is described in Fig. 17. The VTEC based on the estimated receiver bias from the neural network is higher than the VTEC computed by the reference method because the neural network mostly underestimates the receiver bias value. However, the maximum deviations of VTEC in each tested day as shown in Fig. 17 are still acceptable in

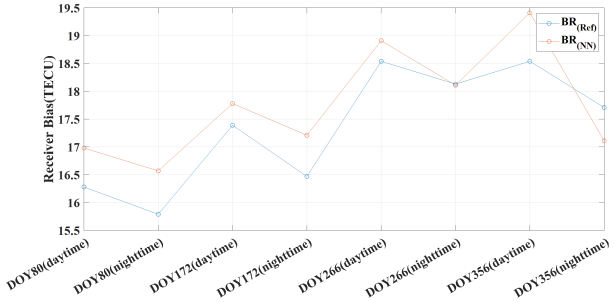

***Fig. 15**: Comparison of the estimated receiver bias between the reference method and the proposed neural network at the KMIT station.*

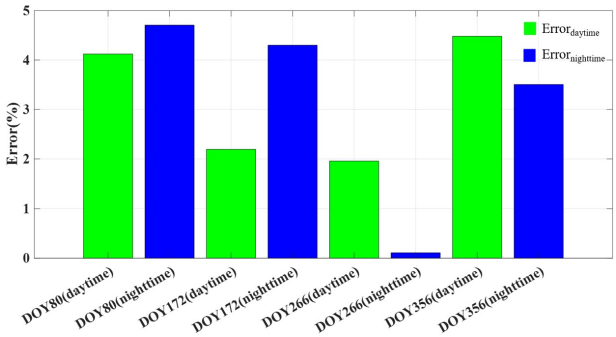

***Fig. 16**: Percentages of errors during testing the neural network model at KMIT station.*

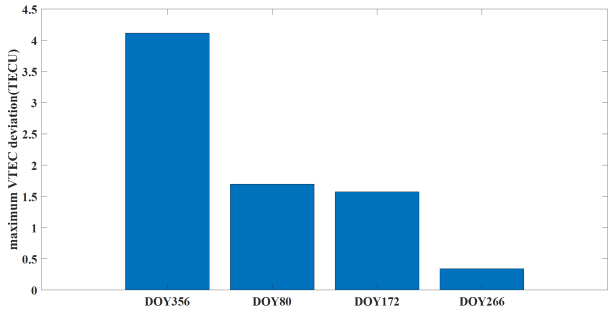

***Fig. 17**: Maximum deviation in VTEC by using receiver biases from neural network approach compared to the reference method at KMIT station.*

most cases such as general TEC Map, Global Ionospheric Maps (GIMs) released by Ionosphere Associate Analysis Centers (IAACs) might have a deviation of approximately 5 TECU in some case[23].

4.3 Prediction at Other Stations

We also examine the prediction performances of the proposed trained model with observation data from another station, AER1 station at the Suvarnabhumi International Airport, Bangkok, which are not the used in the training process. The comparison of the receiver bias from the reference method and the neural network models at AER1 stations is shown in Fig. 18 and the percentages of errors from the baseline reference method

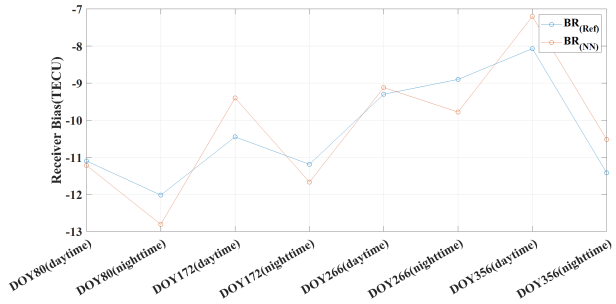

***Fig. 18**: Comparison of the estimated receiver bias between the reference method and the proposed neural network at the AER1 station.*

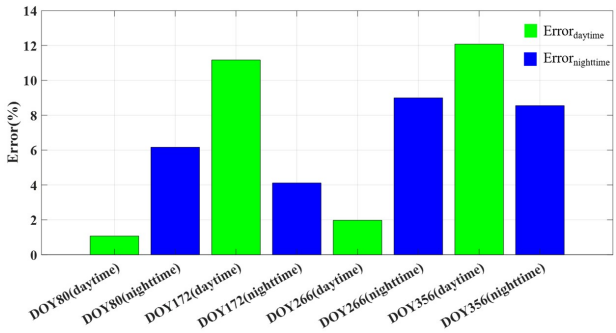

***Fig. 19**: Percentage of errors between receiver bias values from baseline reference method and a neural network (trained by interpolated dataset) at AER1 station.*

in Fig. 19. As we can see in the figures, we can still use the NN model to estimate the receiver bias from the neural network at another station with the slightly higher deviation, around 10 percent in some cases. However, the receiver bias can still follow the trend and it still shows high values during the daytime and low values during the nighttime.

5. CONCLUSION

In this work, the receiver bias is predicted from slant total electron content (STEC) after removing satellite bias using a neural network with the Levenberg-Marquart algorithm over the 3-year datasets of GNSS ground-based receiver stations over Thailand. Two hidden layers are used for the neural network and the model is trained with the various number of neurons. We get the optimal result at 50 neurons in each layer during training. Most predicted receiver biases differ less than 10 percent from the calculated receiver bias by the reference method. The trained neural network model can also predict the receiver bias from other stations which are not part of the training process. The neural model shows faster performance over the baseline reference method when testing on the same hardware and software parameters.

ACKNOWLEDGMENTS

This article is the extended version of the conference paper that was presented at the 19th International Conference on Electrical Engineering Electronics, Computer, Telecommunications, and Information Technology (ECTI-CON), 2022 in Hua Hin, Thailand. The TEC database is obtained from the Thai GNSS and Space Weather Information Data Center. We are thankful to Stamford International University and Aeronautical Radio of Thailand for providing the GNSS data, and Electronics Navigation Research Institute (Japan) providing the GNSS observation equipment. This work is supported by King Mongkut's Institute of Technology Research Fund (Grant no. KREF016422) and The Royal Golden Jubilee (RGJ) Ph.D. Programme (grant number PHD/0166/2561). The ASEAN IVO (http://www.nict.go.jp/en/asean_ivo/ index.html) project, [GNSS and Ionospheric Data Products for Disaster Prevention and Aviation in Magnetic Low-Latitude Regions (Phase II)], was also involved in the production of the contents of this work and financially supported by NICT (http://www.nict.go.jp/en/index.html).

REFERENCES

[1] K. Hozumi, P. Supnithi, S. Lerkvaranyu, T. Tsugawa, T. Nagatsuma, and T. Maruyama, "TEC prediction with neural network for equatorial latitude station in Thailand," *Earth, Planets and Space*, vol. 64, no. 6, pp. 473–483, Jun. 2012.

[2] E. Yizengaw, M. B. Moldwin, D. Galvan, B. A. Iijima, A. Komjathy, and A. J. Mannucci, "Global plasmaspheric TEC and its relative contribution to GPS TEC," *Journal of Atmospheric and Solar-Terrestrial Physics*, vol. 70, no. 11–12, pp. 1541–1548, Aug. 2008.

[3] X. F. Ma, T. Maruyama, G. Ma, and T. Takeda, "Determination of GPS receiver differential biases by neural network parameter estimation method," *Radio Science*, vol. 40, no. 1, Jan. 2005.

[4] D. Sunehra, K. Satyanarayana, C. Viswanadh, and A. Sarma, "Estimation of total electron content and instrumental biases of low latitude global positioning system stations using Kalman filter," *IETE Journal of Research*, vol. 56, no. 5, p. 235, 2010.

[5] E. Sardón and N. Zarraoa, "Estimation of total electron content using GPS data: How stable are the differential satellite and receiver instrumental biases?," *Radio Science*, vol. 32, no. 5, pp. 1899–1910, Sep. 1997.

[6] G. Ma and T. Maruyama, "Derivation of TEC and estimation of instrumental biases from GEONET in Japan," *Annales Geophysicae*, vol. 21, no. 10, pp. 2083–2093, Oct. 2003.

[7] P. Kenpankho, P. Supnithi, and T. Nagatsuma, "Comparison of observed TEC values with IRI-2007 TEC and IRI-2007 TEC with optional foF2 measurements predictions at an equatorial region,

Chumphon, Thailand," *Advances in Space Research*, vol. 52, no. 10, pp. 1820–1826, Nov. 2013.

[8] A. Chiablaem et al., "Estimation of the single GPS-receiver bias using the gradient descent algorithm," *2016 13th International Conference on Electrical Engineering/Electronics, Computer, Telecommunications and Information Technology (ECTI-CON)*, Chiang Mai, Thailand, 2016, pp. 1-5.

[9] B.-K. Choi, J.-U. Park, K. Min Roh, and S.-J. Lee, "Comparison of GPS receiver DCB estimation methods using a GPS network," *Earth, Planets and Space*, vol. 65, no. 7, pp. 707–711, Jul. 2013.

[10] G. Ma, W. Gao, J. Li, Y. Chen, and H. Shen, "Estimation of GPS instrumental biases from small scale network," *Advances in Space Research*, vol. 54, no. 5, pp. 871–882, Sep. 2014.

[11] S. Sahu, R. Trivedi, R. K. Choudhary, A. Jain, and S. Jain, "Prediction of Total Electron Content (TEC) using Neural Network over Anomaly Crest Region Bhopal," *Advances in Space Research*, vol. 68, no. 7, pp. 2919–2929, Oct. 2021.

[12] G. Sivavaraprasad, V. S. Deepika, D. SreenivasaRao, M. Ravi Kumar, and M. Sridhar, "Performance evaluation of neural network TEC forecasting models over equatorial low-latitude Indian GNSS station," *Geodesy and Geodynamics*, vol. 11, no. 3, pp. 192–201, May 2020.

[13] K. Watthanasangmechai, P. Supnithi, S. Lerkvaranyu, T. Tsugawa, T. Nagatsuma, and T. Maruyama, "TEC prediction with neural network for equatorial latitude station in Thailand," *Earth, Planets and Space*, vol. 64, no. 6, pp. 473–483, Jun. 2012.

[14] X. F. Ma, T. Maruyama, G. Ma, and T. Takeda, "Determination of GPS receiver differential biases by neural network parameter estimation method," *Radio Science*, vol. 40, no. 1, Jan. 2005.

[15] H. Tuna, O. Arikan, F. Arikan, T. L. Gulyaeva, and U. Sezen, "Online user-friendly slant total electron content computation from IRI-Plas: IRI-Plas-STEC," *Space Weather*, vol. 12, no. 1, pp. 64–75, Jan. 2014.

[16] G. Ma and T. Maruyama, "Derivation of TEC and estimation of instrumental biases from GEONET in Japan," *Annales Geophysicae*, vol. 21, no. 10, pp. 2083–2093, Oct. 2003.

[17] D. R. Themens, P. T. Jayachandran, and R. B. Langley, "The nature of GPS differential receiver bias variability: An examination in the polar cap region," *Journal of Geophysical Research: Space Physics*, vol. 120, no. 9, pp. 8155–8175, Sep. 2015.

[18] International Association of Geodesy, "International GNSS Service," Jul. 2022.

[19] E. Grossi and M. Buscema, "Introduction to artificial neural networks," *European Journal of Gastroenterology & Hepatology*, vol. 19, pp. 1046–1054, Jan. 2008.

[20] C. D. Souza, "Neural network learning by the levenberg-marquardt algorithm with Bayesian regularization (part 1)." Available on URL: http://crsouza. blogspot. ro/2009/11/neuralnetwork ..., 2009.

[21] P. Kim, *MATLAB Deep Learning*, 2017.

[22] M. H. Gadallah, K. A. Hamid El-Sayed, and K. Hekman, "Intelligent process modelling using Feed-Forward Neural Networks," *International Journal of Manufacturing Technology and Management*, vol. 19, no. 3/4, pp. 128–257, Feb. 2010.

[23] P. Chen, H. Liu, Y. Ma, and N. Zheng, "Accuracy and consistency of different global ionospheric maps released by IGS ionosphere associate analysis centers," *Advances in Space Research*, vol. 65, no. 1, pp. 163–174, Jan. 2020.

Phyo C Thu received the B.Eng. degree Computer Engineering and Information Technology from Yangon Technological University, Yangon, Myanmar, in 2019 and currently studying M.Eng. degree in Electrical and Computer Engineering from the King Mongkut's Institute of Technology Ladkrabang, Bangkok, Thailand, since 2021.

Pornchai Supnithi received the B.S. degree from the University of Rochester, Rochester, NY, USA, in 1995, the M.S. degree from the University of Southern California, Los Angeles, CA, USA, in 1997, and the Ph.D. degree in electrical Engineering from the Georgia Institute of Technology, Atlanta, GA, USA, in 2002.

Since 2015, he has been a full professor at Telecommunication Engineering Department, Faculty of Engineering, King Mongkut's Institute of Technology Ladkrabang. He has published over 50 journal articles, 100 conference papers, and 3 books/chapters. His research interests are in the area of Telecommunications, Ionospheric and GNSS, Data storage, and Engineering Education. His laboratory is maintaining numerous observation stations in Thailand (with ionosonde, beacon receivers, magnetometer, and GNSS receivers) as well as Thai GNSS and Space Weather Information Website (http://iono-gnss.kmitl.ac.th).

Prof. Dr. Pornchai Supnithi was a mid-career Thailand Research Fund scholar from 2013-2015. He previously served as the second Vice President of ECTI Association. Currently, he serves as a subcommittee member in the National Research Council of Thailand (NRCT), International Reference Ionosphere (IRI) Committee (under URSI, COSPAR), and the National GNSS Infrastructure subcommittee, Ministry of Science and Technology, Thailand.

Jirapoom Budtho received the B.E. and M.E. degrees in Telecommunication Engineering and Ph.D. in Electrical Engineering from King Mongkut's Institute of Technology Ladkrabang, Bangkok, Thailand, in 2015, 2017 and 2023, respectively. He is currently a lecturer in School of Engineering, King Mongkut's Institute of Technology Ladkrabang, Thailand.

His research interests include the ionosphere, GBAS technology, GNSS, and Space Weather Information. He is also a member of Thai GNSS and the Space Weather Information Data Center.

Apitep Saekow received his B.E. in computer and information from Toyohashi University, his M.S. in computer science from La Trobe University and Ph.D. in computer engineering from Thammasat University.

He has over 18 years of experience in teaching in Japan, Australia and Thailand and five years working as a dean and an assistant president for various key roles: academic affairs, academic services and external affairs and International Relations at Stamford International University. He is also a government consultant and a researcher in e-Government interoperability projects. He was a researcher of the winner project of e-Asia Award in India. In 2014, he won the Blackboard Catalyst Award on Innovative Blended Learning from US in 2016. Since 2019, he has been the Acting President at Stamford International University, Thailand.

His research interests are Interoperability in e-Government, e-Business, e-Commerce, Research Methodology, Artificial Intelligence, Genetic Algorithms and Education Management.

Thanomsak Sopon is currently Assistant Professor with the Department of Electronics Engineering, Faculty of Engineering and Technology, Rajamangala University of Technology Isan, Nakhonratchasima, Thailand.

His current research interests are in the areas of data storage system, digital signal processing for communications and artificial intelligence.

Kornyanat Hozumi received the M.Eng. degree in telecommunications engineering from the King Mongkut's Institute of Technology Ladkrabang, Bangkok, in 2011, and the Ph.D. degree in informatics from Kyoto University, Kyoto, Japan, in 2015. From May to September 2015, she was a Researcher with the Research Institute for Sustainable Humanosphere (RISH), Kyoto University. Since October 2015, she has been a Researcher with the Space Environment Laboratory, Applied Electromagnetic Research Institute, National Institute of Information and Communications Technology (NICT), Tokyo, Japan. Her research interests include employing radio wave technique to study ionosphere and upper atmosphere and linking the space weather research to the real operation.

Lin Min Min Myint ris currently an Assistant Professor with the King Mongkut's Institute of Technology Ladkrabang, Thailand. He is a member of Thai GNSS and the Space Weather Information Data Center.

His research interests include signal processing on data storage and communications, space weather analysis, and GNSS positioning and navigation.